

Review

Applications of Ni-Based Catalysts in Photothermal CO₂ Hydrogenation Reaction

Zhimin Yuan ¹, Xianhui Sun ², Haiquan Wang ^{1,*}, Xingling Zhao ¹ and Zaiyong Jiang ^{1,*}

¹ School of Chemistry & Chemical Engineering and Environmental Engineering, Weifang University, Weifang 261061, China

² Food and Drug Department, Weifang Vocational College, Weifang 261061, China

* Correspondence: haiquan202@hotmail.com (H.W.); zaiyongjiang@qlu.edu.cn (Z.J.)

Abstract: Heterogeneous CO₂ hydrogenation catalytic reactions, as the strategies for CO₂ emission reduction and green carbon resource recycling, play important roles in alleviating global warming and energy shortages. Among these strategies, photothermal CO₂ hydrogenation technology has become one of the hot catalytic technologies by virtue of the synergistic advantages of thermal catalysis and photocatalysis. And it has attracted more and more researchers' attentions. Various kinds of effective photothermal catalysts have been gradually discovered, and nickel-based catalysts have been widely studied for their advantages of low cost, high catalytic activity, abundant reserves and thermal stability. In this review, the applications of nickel-based catalysts in photothermal CO₂ hydrogenation are summarized. Finally, through a good understanding of the above applications, future modification strategies and design directions of nickel-based catalysts for improving their photothermal CO₂ hydrogenation activities are proposed.

Keywords: photothermal catalysis; Ni-based catalysts; CO₂ hydrogenation; photothermal catalysts

1. Introduction

With the continuous progress of social productivity and science and technology, economic pillar industries such as chemical production, power systems, automobile manufacturing, etc., have experienced rapid development. This has been accompanied by massive consumption of fossil fuels and excessive emissions of the greenhouse gas CO₂ [1–8]. The scientific problem of how to reduce CO₂ emissions to the maximum extent has aroused great attention from all countries and governments, and they have put forward many coping strategies. Many countries have signed provisions such as the Kyoto Treaty and the Paris Agreement to control CO₂ emissions and slow the pace of global warming [9].

In view of the serious impact of the greenhouse gas CO₂ on the global climate and in order to alleviate human dependence on limited fossil energy, scientists have proposed to catalyze CO₂ into high-value-added valuable organics to replace limited fossil resources and reduce the concentration of CO₂ in the atmosphere [10–15]. Due to the high symmetry and chemical inertness of CO₂ molecules, it is necessary to input a large amount of energy to dissociate the C=O double bond in the converting process of CO₂; so, the introduction of catalysis is imperative. In recent years, many CO₂ utilization technologies have been explored and discovered, mainly including photocatalysis, thermal catalysis, electrocatalysis, biological conversion, photothermal catalysis and other methods [16–22]. Photocatalytic CO₂ technology converts CO₂ into methane, carbon monoxide, methanol and other substances under the action of light and semiconductor catalysts. Thermal catalytic conversion of CO₂ converts CO₂ into useful chemicals or fuels by using catalysts under high-temperature conditions. Electrocatalysis refers to the conversion and reduction of CO₂ into renewable energy under the action of electric energy and electrodes. Biological conversion is the conversion of CO₂ into organics and fuels through metabolic methods and other means such as biological methods. Photothermal catalysis of CO₂ is a new direction of



Citation: Yuan, Z.; Sun, X.; Wang, H.; Zhao, X.; Jiang, Z. Applications of Ni-Based Catalysts in Photothermal CO₂ Hydrogenation Reaction. *Molecules* **2024**, *29*, 3882. <https://doi.org/10.3390/molecules29163882>

Academic Editor: Eun Duck Park

Received: 30 July 2024

Revised: 13 August 2024

Accepted: 15 August 2024

Published: 16 August 2024



Copyright: © 2024 by the authors. Licensee MDPI, Basel, Switzerland. This article is an open access article distributed under the terms and conditions of the Creative Commons Attribution (CC BY) license (<https://creativecommons.org/licenses/by/4.0/>).

catalytic conversion driven by solar energy and heat utilized in recent years. Photothermal catalysis includes four types of actions: thermal-assisted photocatalysis (thermal energy improves the separation of photo-generated charge carriers), photo-assisted thermocatalysis (solar energy enhances the local temperature of the catalyst surface), photo-driven thermocatalysis (the catalyst has high light absorption capacity, thereby achieving photo-to-thermal conversion under light irradiation) and photothermal co-catalysis (the catalyst could exhibit contributions to both the thermochemical and photochemical reactions) [23]. Different from thermal catalysis and photocatalysis, it collaboratively drives the catalytic reaction of CO₂ by combining thermocatalysis and photocatalysis, which can usually enhance catalytic activity and selectivity compared to thermally driven reactions [24,25]. Among the above-mentioned CO₂ conversion technologies, photothermal catalytic CO₂ hydrogenation technology is regarded by the majority of scientific researchers as a technology with great application potential, and has received more and more attention [26–30].

Therefore, a large number of CO₂ hydrogenation photothermal catalysts have been explored one after another, showing a very good industrial application prospect in terms of activity. Among them, supported catalysts (metal/oxide) are the hot-topic materials in this field, which are mainly composed of active metals (such as Rh [31], Ru [32,33], Pd [34], Pt [35,36], Cu [37–39], Ni [40], Co [41,42], Fe [43,44], etc. [45]) and metal oxide supports (for instance TiO₂ [46–48], SiO₂ [49], In₂O₃ [50], CeO₂ [51,52], Al₂O₃ [53], etc. [54–56]). Taking into account the high price of precious metals, insufficient reserves and other problems, their large-scale promotion and industrialization is severely limited. From the perspective of large-scale industrial applications, non-precious metals with abundant reserves, cheap costs and good activity (for example, Cu, Ni, Co, etc.) have received ever-increasing attention [57–66]. And their explorations in the field of photothermal CO₂ hydrogenation have gradually deepened in recent years [67–75].

Ni (nickel), despite being one of the hot-topic materials of non-precious metals, to date, there are few review papers reporting on applications of Ni-based catalysts in photothermal CO₂ hydrogenation. To facilitate a deeper and more convenient comprehension for a broader audience of researchers in this field, it is imperative to conduct a comprehensive application review based on recent advances. This review will sum up the photothermal CO₂ hydrogenation applications of Ni-based catalysts in three aspects: photothermal CO₂ methanation, photothermal reverse water–gas reaction (RWGS), and photothermal CO₂ hydrogenation to produce methanol. Based on the above applications, this review presents the research progress, some current problems and challenges, and some strategies to further enhance the activities Ni-based catalysts, and proposes future research directions.

2. Possible Photothermal CO₂ Hydrogenation Reaction Path

The photothermal CO₂ hydrogenation reaction of Ni-based catalysts is a complex multi-step reaction, so its reaction path is complex and uncertain, resulting in the formation of many types of products, such as CO, CH₄ and CH₃OH. The following is a possible and brief statement about the reaction path according to the different products [76–79].

Photothermal reverse water–gas shift reaction (CO₂ + H₂ ⇌ CO + H₂O). The level of hydrogen consumption in the photothermal reverse water–gas shift reaction (RWGS) is the least out of all of the CO₂ hydrogenation reactions. The CO product is the basic raw material for many important industrial products, so it is considered a highly popular reaction. The RWGS reaction includes two main reaction pathways: (1) the CO path. Carbon dioxide is first adsorbed on the surface of the catalyst to form *CO₂ active species. Then, through the direct break of the C–O chemical bond, *CO₂ can be directly converted into *CO and *O. Finally, *CO adsorbed on the catalyst surface produces CO via desorption. (2) The carboxyl (*HOCO) intermediate path. In this process, the CO₂ adsorbed on the catalyst surface (*CO₂) is hydrogenated to form the intermediate species carboxyl group (*HOCO), and then, the *HOCO intermediates are cleaved to form *CO and *OH species at the corresponding active sites. Finally, the *CO intermediates are desorbed from the catalyst surface to form gaseous CO. Regardless of the path, the adsorption capacity of *CO on

the catalyst surface has an important effect on the selectivity of CO. A suitable adsorption capacity is conducive to the formation of CO. A strong adsorption capacity is not favorable for the desorption of *CO, which will cause *CO to continue under hydrogenation, thereby changing the selectivity of CO.

Photothermal CO₂ methanation ($\text{CO}_2 + 4\text{H}_2 \rightleftharpoons \text{CH}_4 + 2\text{H}_2\text{O}$). CO₂ methanation is one of the important reactions to produce methane, which has important practical significance in industrial production. It has been reported that there are two main reaction paths for photothermal CO₂ methanation. The direct cleavage path of the C-O bond. CO₂ is adsorbed on the surface of the catalyst to form *CO₂ active species, which are directly converted into *CO and *O. The formed *CO continues to dissociate to *C and *O, and subsequently, *C can undergo hydrogenation to produce *CH, *CH₂, *CH₃ and *CH₄. *CH₄ is desorbed from the surface of the catalyst to form CH₄. Alternatively, there is the formate pathway. *CO₂ is hydrogenated to produce H_xCO active species, and then, the C-O chemical bonds in H_xCO are broken to form *CH_x. *CH_x can continue to undergo a series of hydrogenation processes to form *CH₄, which is subsequently desorbed from the catalyst surface to form CH₄.

Photothermal methanol production ($\text{CO}_2 + 3\text{H}_2 \rightleftharpoons \text{CH}_3\text{OH} + \text{H}_2\text{O}$). As we all know, methanol is an important chemical raw material and hydrogen storage material, which makes the research on photothermal catalytic CO₂ hydrogenation for methanol production the object of much attention. According to research reports, there are two main reaction paths for photothermal CO₂ hydrogenation for methanol production at present. (1) The *CO intermediate path. *CO₂ first undergoes the RWGS reaction to produce *CO, which can be continuously hydrogenated to produce CH₃OH. (2) The formate pathway (*HCOO). *CO₂ is hydrogenated to produce *H₂COOH, which can be converted to CH₃OH by breaking the C-O chemical bond and undergoing hydrogenation. It seems that the description is very simple, but in fact, the whole reaction process is complex and may also involve the conversion of many other intermediates.

3. Photothermal CO₂ Hydrogenation Applications of Ni-Based Catalysts

3.1. Photothermal Reverse Water–Gas Reaction

The photothermal reverse water–gas reaction is a promising candidate for efficient utilization of CO₂ and hydrogen energy. However, the conversion rate of carbon dioxide is limited by the thermodynamic equilibrium. It is a hot topic to explore photothermal catalysts with high activity, high CO selectivity and high CO₂ conversion. In the early stage, Pt, Pd and some precious metals were found to have good catalytic activities in the RWGS reaction [36]. In recent years, considering the price and reserves of precious metals, the exploration of non-precious metal catalysts has become more and more extensive [80]. Among them, Ni-based catalysts have attracted great interest because of their abundant reserves, low price and good catalytic activity [81].

However, after more than ten years of exploration, it has been found that the CO selectivity of Ni-based catalysts is not high when performing RWGS, and there is always a large number of CH₄ by-products which interfere. A lot of effort has been put into exploring the high selectivity of CO. For example, Song et al. discovered that single atoms of Ni can cause Pauli incompatibility through theoretical calculations, thereby preventing the formation of CO by-products in the process of RWGS [82]. Based on their calculations, in this study, nickel was loaded onto the surface of CeO₂ nanosheets to explore the catalytic activity and selectivity of photothermal CO₂ hydrogenation. By XRD characterization (Figure 1a), no diffraction peaks of Ni were found, indicating that Ni particles are very small. It was determined by TEM (Figure 1b) that Ni particles belong to the atomic level. Atomically, Ni/CeO₂ underwent the photothermal RWGS reaction, and the results are shown in Figure 1c,d. It is evident that atomically, Ni/CeO₂ exhibits 100% CO selectivity and has a good catalytic rate (23.1 mmol·g⁻¹·h⁻¹). By analyzing the XPS spectra of the samples before and after the RWGS reaction, it is found that the valence state of Ni is stable at the oxidation state +2 valence. It can be seen that the Ni active species on the catalyst surface have an important effect on the CO selectivity of the RWGS reaction.

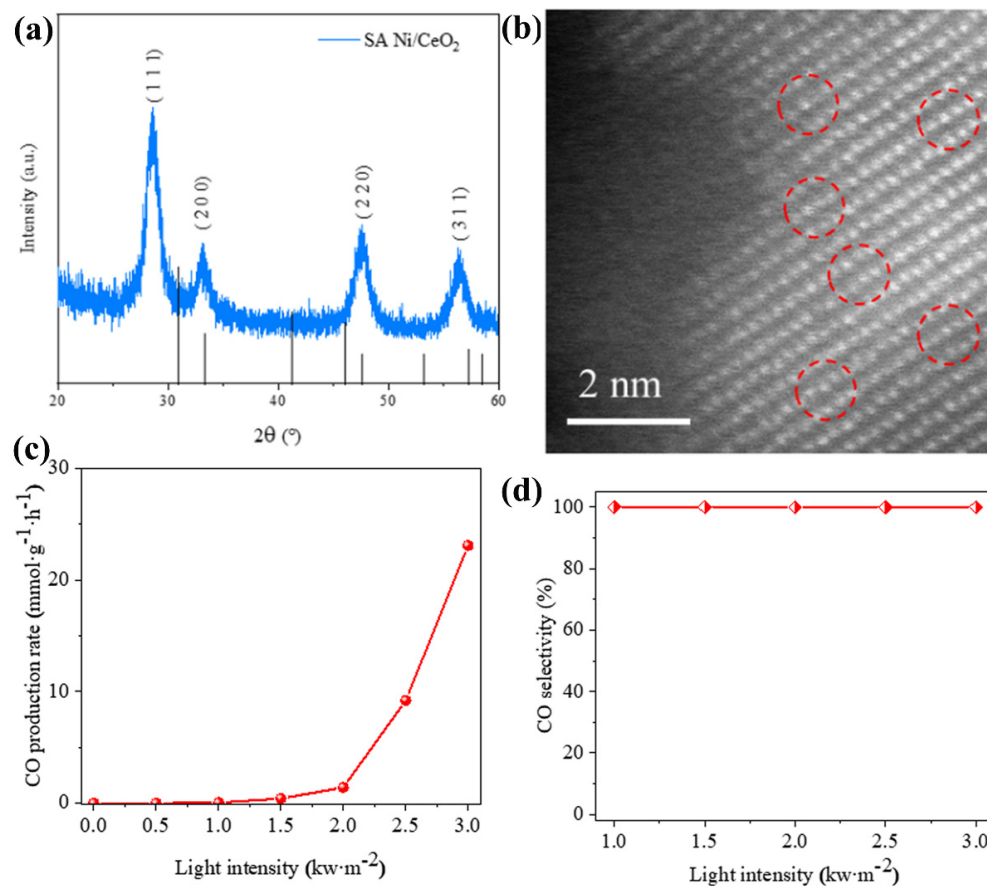


Figure 1. (a) The XRD image and (b) TEM image of atomic Ni/CeO₂. (c) The CO production rate and (d) CO selectivity of atomic Ni/CeO₂ under varying sunlight irradiation. Reprinted with permission from Ref. [82]. Copyright 2023, Elsevier B.V.

In addition, the support of Ni-based catalysts also has an important effect on the RWGS reaction. For example, researchers have explored significant differences between CeO₂ and N-doped CeO₂ [83]. Based on the XRD image (Figure 2a), it can be found that the diffraction peak of Ni/CeO₂ is shifted to a lower angle after nitrogen doping, which confirms the successful doping of N. The photothermal catalytic CO₂ hydrogenation activity diagrams (Figure 2b) show that the CO selectivity of Ni/CeO₂ is only 30%, while the CO selectivity of Ni/N_x-CeO₂ is almost 100%. And the CO yields of the Ni/N_x-CeO₂ samples are improved compared to those of Ni/CeO₂. In addition, the cyclic reaction exhibited that the catalytic activity has no decrease (Figure 2c), suggesting that the Ni/N_x-CeO₂ composite possesses excellent stability. Through XPS (Figure 2d) and in situ FT-IR characterization, the researchers found that N-H chemical bonds appear on the surface of Ni/N_x-CeO₂ after the photothermal RWGS reaction, which reduces the number of active *H species. It was found by theoretical calculation that the ability of Ni/N_x-CeO₂ to break down hydrogen is weaker than that of Ni/CeO₂. These results indicate that changes in selectivity are significantly associated with the formation of N-H chemical bonds. The Gibbs free energy calculation results show that *CO is more easily desorbed from the surface of Ni/N_x-CeO₂ than Ni/CeO₂, thereby being more conducive to CO generation. Moreover, the alloying strategy is also an effective method to increase CO selectivity in the photothermal CO₂ hydrogenation reaction of Ni-based catalysts. The researchers found that a Ni-Mo alloy can regulate the selectivity of CO in photothermal CO₂ hydrogenation, and even Ni1Mo1 can obtain 98% CO selectivity [77]. The studies show that Mo can regulate the electronic structure of Ni, weaken the ability of Ni to decompose hydrogen and increase the desorption of *CO from the surface of the catalyst, which is the main cause of the formation of CO.

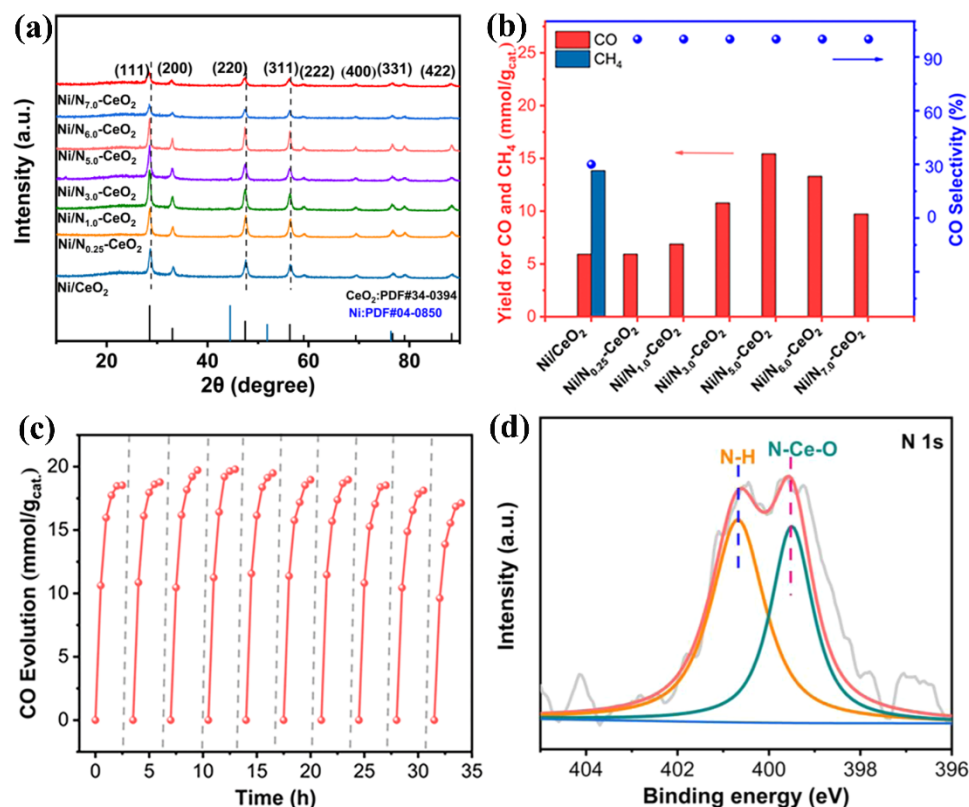


Figure 2. (a) XRD images of samples, (b) photothermal CO₂ hydrogenation activities of samples, (c) cyclic reaction of Ni/N_{5.0}-CeO₂, and (d) XPS spectrum of N 1s in Ni/N_{5.0}-CeO₂ after reaction. Reprinted with permission from Ref. [83]. Copyright 2021, American Chemical Society.

3.2. Photothermal CO₂ Methanation

In 1897, Paul Sabatier experimentally confirmed the CO₂ methanation reaction. After more than 120 years of exploration and research, CO₂ methanation (that is, the Sabatier reaction) technology has been better expanded and developed. CH₄ (methane) is a key component of natural gas, which is a high-quality energy source and has great potential to replace coal as a clean fuel. In addition, it can also be used as a chemical raw material for the production of acetylene, carbon black, methane chloride and other chemical products. Therefore, it has gradually become a strategic resource and aroused widespread interest globally among researchers. Currently, thermal catalytic CO₂ methanation has been used commercially on a large scale [84]. However, due to the high stability of CO₂ molecules, high temperature and high pressure are needed to achieve efficient conversion, which leads to high energy consumption, environmental problems and harsh reaction conditions. It is of great significance to use renewable and clean energy to promote CO₂ methanation under milder and more environmentally friendly conditions. Solar energy is a non-polluting, sustainable renewable energy source, and has been regarded as a viable auxiliary thermal catalytic CO₂ methane energy source. Therefore, photothermal catalytic CO₂ methanation technology has become one of the hot technologies because of its advantages such as mild reaction conditions, low energy consumption, green environmental protection capacity and good performance [84]. A large number of CO₂ methanation photothermal catalysts have been explored, showing a very good prospect of industrial application in terms of activity. In particular, Ni-based catalysts have been considered promising materials and have been extensively explored [85,86].

For instance, Li et al. obtained TiO₂ with a large specific surface area by converting MIL-125 (Ti-MOFs) and then loaded Ni particles with a smaller size and better dispersion on its surface, compared to using P25 (Figure 3a,b) [87]. Through the photothermal CO₂ methanation reaction (Figure 3c,d), it can be seen that the catalytic activity of pure TiO₂ is

very low, and the introduction of nickel can greatly improve its catalytic activity. In addition, Ni/TiO₂ exhibits a higher CO₂ conversion rate than Ni/P25, and its methane selectivity is close to 99%. A series of characterization tests confirmed that a large specific surface area is conducive to the adsorption and activation of carbon dioxide, and highly dispersed nickel particles can provide more surface-active sites for CO₂ methanation. Ni/TiO₂ has stronger interfacial interactions than Ni/P25, thereby increasing the density of Ni electronic states on the surface of Ni/TiO₂, which is conducive to improving the ability of Ni to decompose H₂ and CO₂. It can be seen from this work that the size, dispersion and surface electron state density of nickel particles play important roles in the photothermal CO₂ methanation reaction.

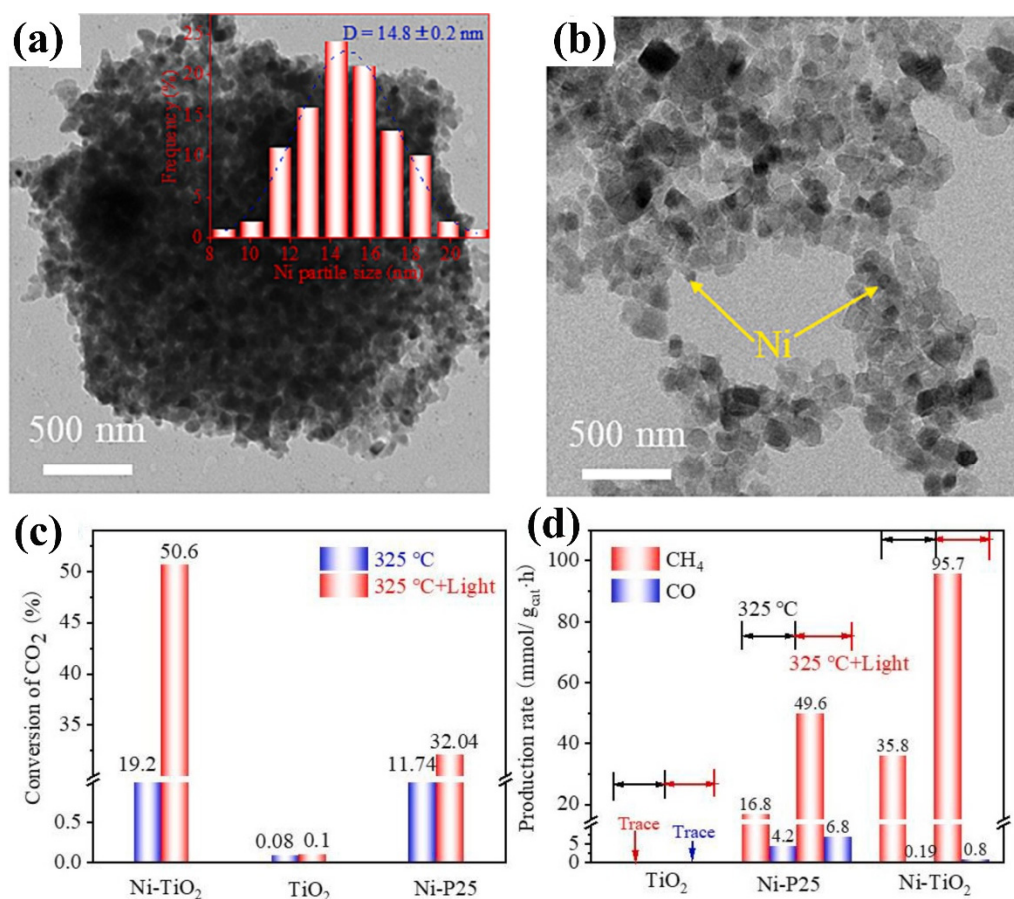


Figure 3. (a,b) The TEM image of Ni/TiO₂. (c) The CO₂ conversion and (d) production rate of the samples [87]. Copyright 2023, Elsevier B.V.

In addition, metal support interactions (MSIs) play an important role in regulating the photothermal CO₂ methanation of Ni-based catalysts. For example, Li et al. used titanium dioxide supports of different sizes to effectively regulate the SMI between Ni and TiO₂ [78]. It is found that the smaller size of TiO₂ exhibits a stronger SMI. The main reason is that the smaller size of TiO₂ has more sufficient oxygen vacancies on the surface, so the Ni atoms can be further effectively anchored, increasing the compatibility between the two. With the enhancement of SMI, photo-generated electrons by TiO₂ excitation can easily migrate to the surface of Ni particles. The high electron density of Ni can promote the dissociation capacity of H₂ molecules and the adsorption capacity of *CO intermediates, so that CO can undergo a deep hydrogenation reaction, resulting in the high selectivity of CH₄. On the contrary, the SMI of large-sized TiO₂ particles is weak, the adsorption capacity of the catalysts for *CO intermediates is insufficient, and it is easy for them to desorb and directly generate CO, resulting in the reduction in CH₄ selectivity. As shown in Figure 4a,b, it can be clearly found that Ni/TiO₂-25 (support size is about 25 nm) shows a

higher CH₄ selectivity than Ni/TiO₂-100 (support size is about 100 nm). The reaction path is that TiO₂ photoelectrons migrate to Ni particles to form Ni⁻ under ultraviolet-visible light irradiation; the left holes in TiO₂ can assist H₂ molecules to transform into H⁺ ions. Then, H⁺ combines with Ni⁻ to form Ni-H active species, which react with *CO₂ to form many intermediates such as HCO*, H₂CO*, H₃CO* and so on. Finally, the C-O bonds of the above intermediates are broken to form CH₄.

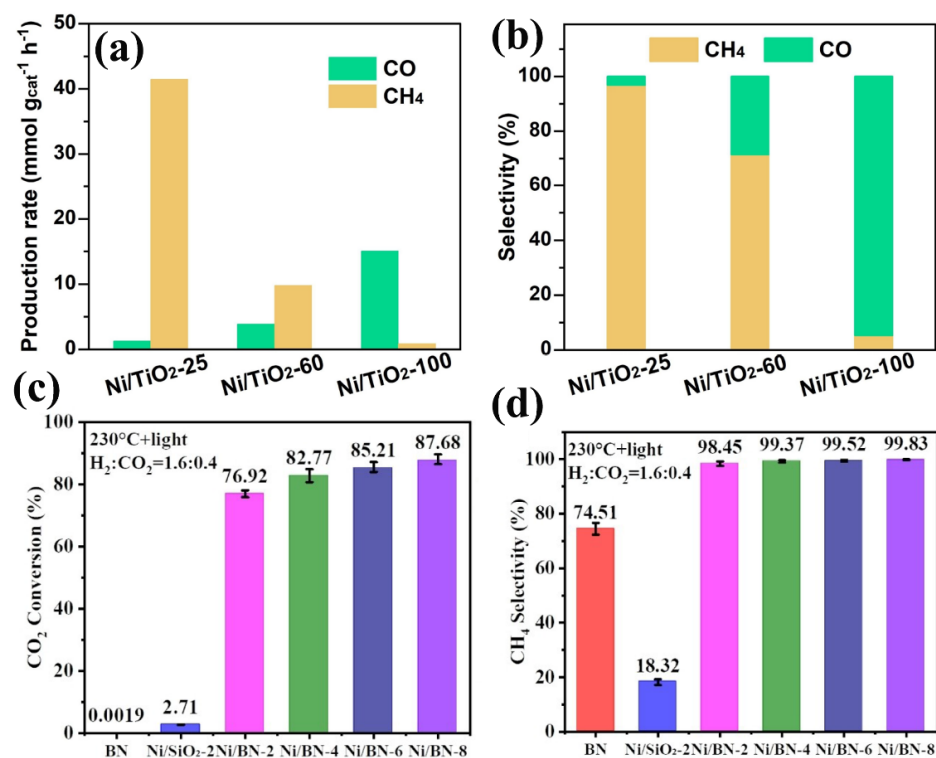


Figure 4. (a) The production rate and (b) selectivity images of the samples. (c) The CO₂ conversion and (d) CH₄ selectivity of the samples. Reprinted with permission from Ref. [78]. Copyright 2024, Wiley. Reprinted with permission from Ref. [79]. Copyright 2023, Wiley.

Moreover, the CO₂ adsorption and activation of Ni-based catalysts are also important factors limiting the rate and selectivity of CO₂ methanation. When the CO₂ adsorption capacity of the catalyst is poor, CO₂ will not be fully adsorbed on the active site, and the activation capacity of CO₂ will be low, which will lead to an insufficient reaction concentration and a high CO₂ conversion energy barrier, and may even cause changes in the type of intermediates and reaction path, thus limiting the reaction rate and selectivity. The developed “Frustrated Lewis Pairs” (FLPs) chemistry in recent years provides a useful approach and method for enhancing the design of CO₂ chemisorption and activation capacities of catalysts. FLPs are generally composed of a pair of Lewis acid sites and Lewis base sites within or between molecules, but due to the obstruction of spatial coordination, these two active sites cannot form traditional Lewis acid–base admixtures, so they show some special chemical properties and catalytic activities. This theory gives us a new revelation: using this FLP chemical method constructs an active interface on the surface of the support, so as to significantly improve the CO₂ adsorption and activation ability of the catalyst, which is a new strategy different from previous design ideas (the many existing methods are physical actions such as concepts of regulating the specific surface area and pore size, bonding activated carbon with a high CO₂ adsorption capacity, adjusting the crystal plane, etc.). This method is promising to further improve the catalytic activity of CO₂ methanation of nickel-based catalysts. Based on the above ideas, Jiang et al. constructed HOB⋯B FLPs on the surface of BN [79], and found that Ni/BN showed 87.68% CO₂ methanation conversion, the reaction rate reached 2.03 mol g_{Ni}⁻¹ h⁻¹, and the selectivity

of CH_4 was almost 100% (Figure 4c,d). The results show that FLPs can cooperate with Ni to capture and activate CO_2 and H_2 , so as to perfectly convert CO_2 into CH_4 .

3.3. Photothermal CO_2 Hydrogenation for Methanol Production

Methanol is one of the most important basic raw materials in the chemical industry, which is mainly used for the production of formaldehyde, dimethyl ether, acetic acid olefin (ethylene, propylene), aromatic (benzene, toluene, xylene), gasoline and other organic chemical products or fuels. It could partially alleviate the dependence on petroleum resources. Photothermal CO_2 hydrogenation for methanol production can recycle carbon resources, thereby gradually eliminating the dependence on the decreasing fossil energy sources, which is of great significance to the sustainable development of human society. Ni-based catalysts are also a series of key materials for photothermal CO_2 hydrogenation for methanol production. For example, Zhang et al. explored the application of Ni- In_2O_3 in photothermal CO_2 hydrogenation for methanol production [88]. Firstly, Ni was doped into the crystal lattice of In_2O_3 using the co-precipitation method, and then, a highly dispersed distribution of Ni^0 on the surface of In_2O_3 via reduction pretreatment was achieved. The introduction of Ni increased the oxygen vacancy concentration of In_2O_3 and expanded its light absorption capacity (Figure 5a). The increase in oxygen vacancy is conducive to the adsorption capacity of CO_2 (Figure 5b), and the enhancement of its light absorption capacity can provide more energy and charge carriers for the reaction. Ni is in favor of H_2 dissociation and can provide more H^* active species for the reaction. Therefore, in the photothermal CO_2 hydrogenation reaction, 10%Ni- In_2O_3 shows a higher CO_2 conversion rate (Figure 5c) and a significantly increased methanol generation rate (Figure 5d) compared to pure In_2O_3 . It can be seen from the above results that Ni can boost the methanol production rate of the catalyst with the reaction of photothermal CO_2 hydrogenation for methanol production.

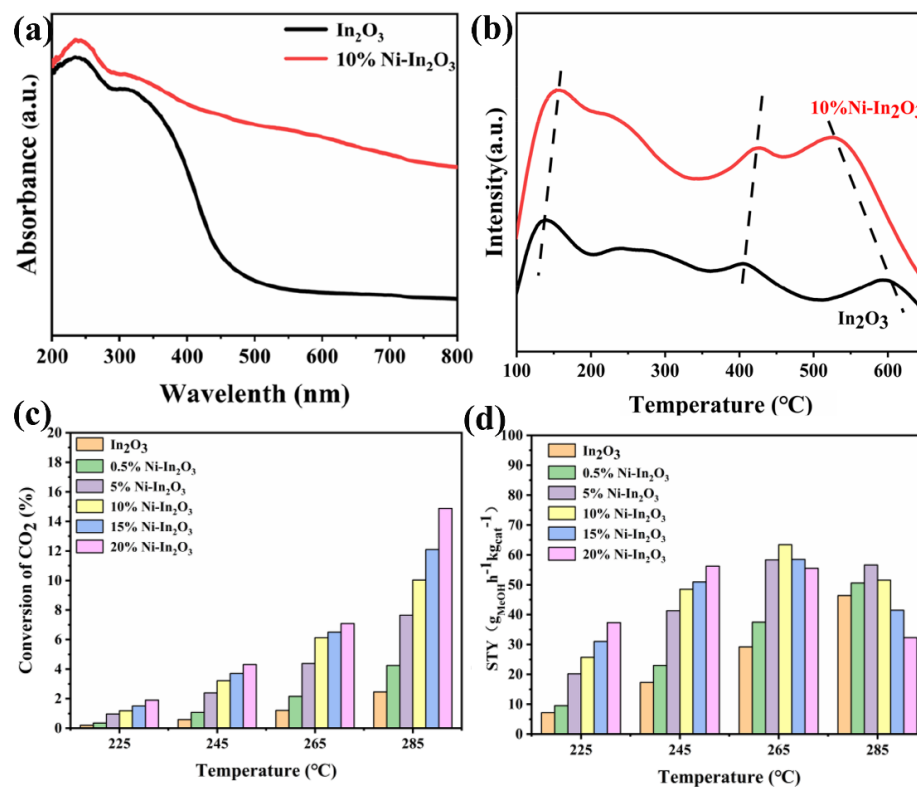


Figure 5. (a) The light absorption and (b) CO_2 TPD images of In_2O_3 and 10%Ni- In_2O_3 . (c) The CO_2 conversion and (d) methanol yield of the samples. Reprinted with permission from Ref. [88]. Copyright 2024, American Chemical Society.

4. In Situ FT-IR Spectra Characterization

In the photothermal CO₂ hydrogenation reaction, a large number of Ni-based catalysts have been explored, but it is a great challenge to design them with the desired activity and selectivity due to the lack of understanding of the internal reaction process and the detailed mechanism of CO₂ hydrogenation. In order to further explore the mystery of photothermal CO₂ hydrogenation of Ni-based catalysts, in situ Fourier Transform infrared (FT-IR) spectra were used to detect the transient kinetic process of this reaction. Recently, Zhang et al. monitored the reaction process of NiMo alloys by using in situ FT-IR spectra while performing their photothermal CO₂ hydrogenation test [77]. As shown in Figure 6, CO₂ molecules adsorbed on the surface of NiMo alloys can be found to exist in the form of bicarbonate (HCO₃⁻) species and monodentate carbonate (m-CO₃²⁻). Their corresponding peaks are located at 1540 and 1650, and 1519, 1470 and 1704 cm⁻¹. In addition, the peaks at 2110 cm⁻¹ could be attributed to the *CO species, and the signals of *CH_x have not been detected throughout the supervision process. The in situ FT-IR spectra indicate that the photothermal CO₂ hydrogenation process of NiMo alloys takes the *CO path, and the experimental results confirm the high CO selectivity mechanism. It can be seen from this study that in situ FT-IR spectra technology plays an important role in the in-depth study of the photothermal CO₂ hydrogenation process of Ni-based catalysts, and it has become a necessary characterization method in this research field.

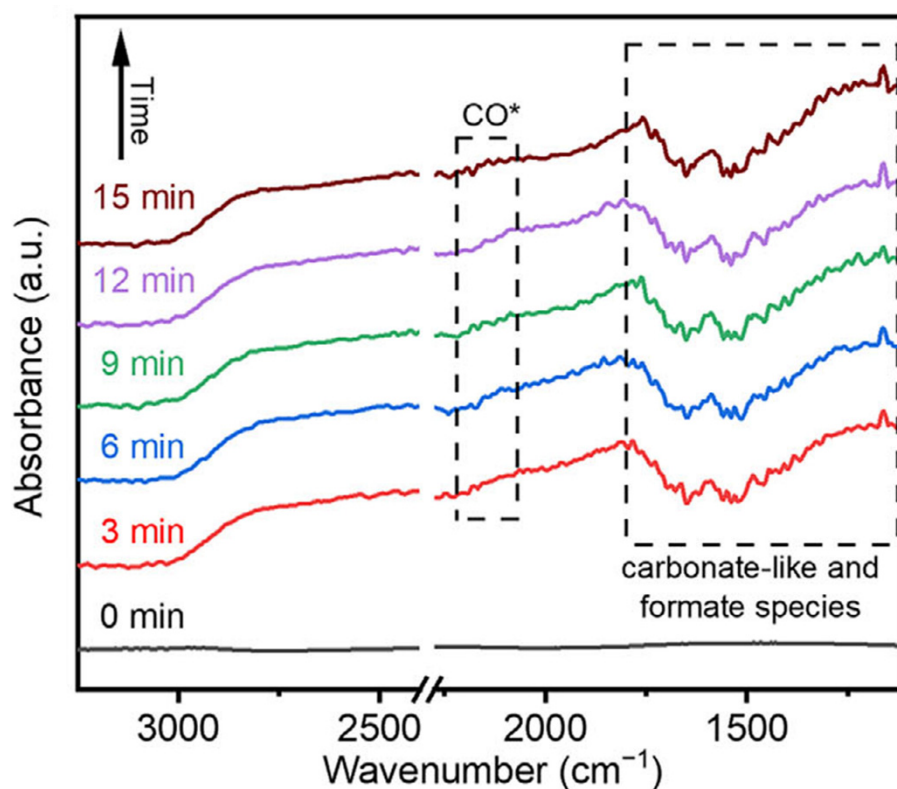


Figure 6. In situ FT-IR spectra of CO₂ photothermal reduction of NiMo alloy in infrared reactor flowing under light irradiation. Reprinted with permission from Ref. [77]. Copyright 2024, Wiley.

5. Future Perspectives and Summary

With the continuous progress of social productivity and science and technology, the energy crisis and environmental pollution has aroused great attention from all countries and governments, and they have put forward many coping strategies. Photothermal CO₂ hydrogenation technology is considered a very good and promising solution to solve the above-mentioned environmental challenges. The key of the above application is suitable catalysts. Among all kinds of catalysts, Ni-based catalysts have become a

series of hot-topic materials due to their advantages of low price, high catalytic activity, good stability and sufficient reserves. Their explorations in the field of photothermal CO₂ hydrogenation have gradually deepened in recent years. Much research work has been conducted to further improve their photothermal catalytic efficiency and product selectivity for meeting practical application requirements. In this review, we summarized the relatively comprehensive photothermal CO₂ hydrogenation applications of Ni-based catalysts, including photothermal CO₂ methanation, the photothermal reverse water–gas reaction (RWGS), and photothermal CO₂ hydrogenation for methanol production. Based on the above applications, this review presents the current research progress and the common reaction path. Many strategies have further enhanced the activities and product selectivity of Ni-based catalysts, but some current problems and challenges need be further studied or optimized, thereby directing future research.

- (1) Currently, the main products of photothermal CO₂ hydrogenation of Ni-based catalysts are CO, CH₄ and CH₃OH. With the deepening of research, it could be found that C₂₊ hydrocarbons are more valuable, but the current research progress and technical capabilities are not able to achieve this goal. In the explorations of some other classes of catalysts, related studies are gradually emerging. It can be observed that the main reaction process of C₂₊ hydrocarbon product production is the *CO-*CH₂ pathway. *CO₂ adsorbed on the catalyst surface forms *CO, which produces *CH₂ by dissociation and hydrogenation of the C-O chemical bond. Then, *CH₂ achieves C-C coupling under the action of a metal catalyst to obtain the generation of C₂₊ hydrocarbon products. Based on the above reaction path principle, Ni-based catalysts can be designed and explored to achieve the production of C₂₊ high-value-added hydrocarbons.
- (2) Recently reported in the journal *Science*, when the catalyst in the CO₂ hydrogenation reaction has 100% selectivity for CO and does not waste hydrogen to produce by-product methane, the RWGS reaction can better achieve the overall carbon negative benefit and simplify the downstream separation process. Therefore, the CO selectivity of Ni-based catalysts in the photothermal RWGS reaction needs to be improved. It is necessary to further modify the Ni-based catalyst or regulate the reaction system. In addition, some design ideas of organic catalysts can also be used for reference, which could do with some experimentation [89,90].
- (3) The hydrogen spillover effect plays an important role in the photothermal CO₂ hydrogenation reaction, but the current research mainly focuses on improving the catalytic activity by regulating the adsorption and activation capacities of CO₂ and H₂, and has neglected the hydrogen spillover effect. Therefore, in future studies, the mechanism of the hydrogen spillover effect should be explored in detail and applied for the improvement in the activity or selectivity of products.
- (4) Due to the strong exothermic reaction and the eight-electron reduction process required for CO₂ methanation, achieving its thermodynamic and kinetic reaction is a great challenge. The temperature is too low, the CO₂ methanation reaction speed is slow, the high temperature will change the reaction balance and the CO₂ conversion rate is low, which do not meet the needs of actual production. At present, few Ni-based catalysts can simultaneously meet the four high production needs of high rate, high conversion, high selectivity and high stability. Therefore, exploring and researching suitable low-temperature catalysts to reduce the energy barrier of CO₂ conversion, accelerate the methane generation rate at a lower or more appropriate temperature, and ensure high CO₂ conversion, high selectivity, high stability and low cost has become a key issue in this field.

Author Contributions: Z.Y.: design, writing and editing original draft. X.S.: writing—review. H.W.: writing—review and editing. X.Z.: writing—review. Z.J.: writing—review and editing. All authors have read and agreed to the published version of the manuscript.

Funding: This study was financially supported by the China Postdoctoral Science Foundation (2020M670483), the Natural Science Foundation of Shandong Province, China (ZR2021QB129, ZR2023MB049), and the Doctoral Research Foundation of Weifang University (2022BS11, 2022BS09).

Data Availability Statement: The data will be made available on request.

Conflicts of Interest: The authors declare that they have no known competing financial interests.

References

1. Zhang, K.; Xu, C.P.; Zhang, X.J.; Huang, Z.Y.; Pian, Q.X.; Che, K.H.; Cui, X.K.; Hu, Y.R.; Xuan, Y.M. Structural Heredity in Catalysis: CO₂ Self-Selective CeO₂ Nanocrystals for Efficient Photothermal CO₂ Hydrogenation to Methane. *Small* **2023**, *20*, 2308823. [CrossRef]
2. Peng, Y.; Szalad, H.; Nikacevic, P.; Gorni, G.; Goberna, S.; Simonelli, L.; Albero, J.; López, N.; García, H. Co-doped hydroxyapatite as photothermal catalyst for selective CO₂ hydrogenation. *Appl. Catal. B Environ.* **2023**, *333*, 122790. [CrossRef]
3. Elavarasan, M.; Yang, W.; Velmurugan, S.; Chen, J.N.; Chang, Y.T.; Yang, T.C.K.; Yokoi, T. In-situ infrared investigation of m-TiO₂/α-Fe₂O₃ photocatalysts and tracing of intermediates in photocatalytic hydrogenation of CO₂ to methanol. *J. CO₂ Util.* **2022**, *56*, 101864. [CrossRef]
4. Mateo, D.; Albero, J.; Garcia, H. Titanium-perovskite-supported RuO₂ nanoparticles for photocatalytic CO₂ methanation. *Joule* **2019**, *3*, 1949–1962. [CrossRef]
5. Yan, T.; Li, N.; Wang, L.; Ran, W.; Duchesne, P.N.; Wan, L.; Nguyen, T.N.; Wang, L.; Xia, M.; Ozin, G.A. Bismuth atom tailoring of indium oxide surface frustrated Lewis pairs boosts heterogeneous CO₂ photocatalytic hydrogenation. *Nat. Commun.* **2020**, *11*, 6095. [CrossRef]
6. Song, H.; Ye, J. Photothermal tandem catalysis for CO₂ hydrogenation to methanol. *Chem* **2022**, *8*, 1181–1183. [CrossRef]
7. Li, Z.; Liu, J.; Shi, R.; Waterhouse, G.I.N.; Wen, X.D.; Zhang, T. Fe-Based Catalysts for the Direct Photohydrogenation of CO₂ to Value-Added Hydrocarbons. *Adv. Energy Mater.* **2021**, *11*, 2002783. [CrossRef]
8. Deng, B.; Song, H.; Peng, K.; Li, Q.; Ye, J. Metal-organic framework-derived Ga-Cu/CeO₂ catalyst for highly efficient photothermal catalytic CO₂ reduction. *Appl. Catal. B Environ.* **2021**, *298*, 120519. [CrossRef]
9. Chu, S.; Majumdar, A. Opportunities and challenges for a sustainable energy future. *Nature* **2012**, *488*, 294–303. [CrossRef]
10. Ma, J.; Yu, J.; Chen, G.; Bai, Y.; Liu, S.; Hu, Y.; Al-Mamun, M.; Wang, Y.; Gong, W.; Liu, D.; et al. Rational design of N-doped carbon-coated cobalt nanoparticles for highly efficient and durable photothermal CO₂ conversion. *Adv. Mater.* **2023**, *35*, 2302537. [CrossRef]
11. Gu, Y.; Ding, J.; Tong, X.; Yao, H.; Yang, R.; Zhong, Q. Photothermal catalyzed hydrogenation of carbon dioxide over porous nanosheet Co₃O₄. *J. CO₂ Util.* **2022**, *61*, 102003. [CrossRef]
12. Jin, B.; Ye, X.; Zhong, H.; Jin, F.; Hu, Y.H. Enhanced photocatalytic CO₂ hydrogenation with wide-spectrum utilization over black TiO₂ supported catalyst. *Chin. Chem. Lett.* **2022**, *33*, 812–816. [CrossRef]
13. Qi, Y.; Jiang, J.; Liang, X.; Ouyang, S.; Mi, W.; Ning, S.; Zhao, L.; Ye, J. Fabrication of black In₂O₃ with dense oxygen vacancy through dual functional carbon doping for enhancing photothermal CO₂ hydrogenation. *Adv. Funct. Mater.* **2021**, *31*, 2100908. [CrossRef]
14. Fang, Y.L.; Zhu, G.H.; Jiang, J.Z.; Yang, L.; Deng, F.X.; Arramel, Li, X. A review of updated S-scheme heterojunction photocatalysts. *J. Mater. Sci. Technol.* **2024**, *177*, 142–180.
15. Wang, L.; Dong, Y.; Yan, T.; Hu, Z.; Ali, F.M.; Meira, D.M.; Duchesne, P.N.; Loh, J.Y.Y.; Qiu, C.; Storey, E.E.; et al. Black indium oxide a photothermal CO₂ hydrogenation catalyst. *Nat. Commun.* **2020**, *11*, 2432. [CrossRef]
16. Ding, X.; Liu, W.X.; Zhao, J.H.; Wang, L.; Zou, Z.G. Photothermal CO₂ Catalysis toward the Synthesis of Solar Fuel: From Material and Reactor Engineering to Techno-Economic Analysis. *Adv. Mater.* **2024**, *23*, 12093. [CrossRef]
17. Belinchón, A.; Hernández, E.; Navarro, P.; Palomar, J. A step closer to sustainable CO₂ conversion: Limonene carbonate production driven by ionic liquids. *J. Clean. Prod.* **2024**, *460*, 142587. [CrossRef]
18. Jiang, Z.Y.; Zhang, X.H.; Sun, W.; Yang, D.R.; Duchesne, P.N.; Gao, Y.G.; Wang, Z.Y.; Yan, T.J.; Yuan, Z.M.; Yang, G.H.; et al. Building a Bridge from Papermaking to Solar Fuels. *Angew. Chem. Int. Ed.* **2019**, *58*, 14850–14854. [CrossRef]
19. Yuan, Z.M.; Zhu, X.L.; Gao, X.Q.; An, C.H.; Wang, Z.; Zuo, C.; Dionysiou, D.D.; He, H.; Jiang, Z.Y. Enhancing photocatalytic CO₂ reduction with TiO₂-based materials: Strategies, mechanisms, challenges, and perspectives. *Environ. Sci. Ecotechnol.* **2024**, *20*, 100368. [CrossRef] [PubMed]
20. Price, C.A.H.; Reina, T.R.; Liu, J. Engineering heterogeneous catalysts for chemical CO₂ utilization: Lessons from thermal catalysis and advantages of yolk@shell structured nanoreactors. *J. Energy Chem.* **2021**, *57*, 304–324. [CrossRef]
21. Gao, J.J.; Shiong, S.C.S.; Liu, Y. Reduction of CO₂ to chemicals and Fuels: Thermocatalysis versus electrocatalysis. *Chem. Eng. J.* **2023**, *472*, 145033. [CrossRef]
22. Rao, Y.; Chibwe, K.; Mantilla-Calderon, D.; Ling, F.Q.; He, Z. Meta-analysis of biogas upgrading to renewable natural gas through biological CO₂ conversion. *J. Clean. Prod.* **2023**, *426*, 139128. [CrossRef]
23. Gao, W.; Li, Y.W.; Xiao, D.Q.; Ma, D. Advances in photothermal conversion of carbon dioxide to solar fuels. *J. Energy Chem.* **2023**, *83*, 62–78. [CrossRef]

24. Wang, Z.J.; Song, H.; Liu, H.; Ye, J. Coupling of solar energy and thermal energy for carbon dioxide reduction: Status and prospects. *Angew. Chem. Int. Ed.* **2020**, *59*, 8016–8035. [[CrossRef](#)]
25. Meng, X.; Wang, T.; Liu, L.; Ouyang, S.; Li, P.; Hu, H.; Kako, T.; Iwai, H.; Tanaka, A.; Ye, J. Photothermal conversion of CO₂ into CH₄ with H₂ over Group VIII nanocatalysts: An alternative approach for solar fuel production. *Angew. Chem. Int. Ed.* **2014**, *53*, 11478–11482. [[CrossRef](#)]
26. Li, N.X.; Liu, M.; Yang, B.; Shu, W.X.; Shen, Q.H.; Liu, M.C.; Zhou, J.C. Enhanced Photocatalytic Performance toward CO₂ Hydrogenation over Nanosized TiO₂-Loaded Pd under UV Irradiation. *J. Phys. Chem. C* **2017**, *121*, 2923–2932. [[CrossRef](#)]
27. Wu, D.D.; Deng, K.X.; Hu, B.; Lu, Q.Y.; Liu, G.L.; Hong, X.L. Plasmon-Assisted Photothermal Catalysis of Low-Pressure CO₂ Hydrogenation to Methanol over Pd/ZnO Catalyst. *ChemCatChem* **2019**, *11*, 1598–1601. [[CrossRef](#)]
28. Song, C.Q.; Wang, Z.H.; Zhao, J.W.; Qin, X.T.; Peng, M.; Gao, Z.R.; Xu, M.; Xu, Y.; Yan, J.; Bi, Y.P.; et al. Photothermal conversion of CO₂ into lower olefins at the interface of the K-promoted Ru/Fe₃O₄ catalyst. *Chem Catal.* **2024**, *4*, 100960. [[CrossRef](#)]
29. Deng, B.W.; Song, H.; Wang, Q.; Hong, J.N.; Song, S.; Zhang, Y.W.; Peng, K.; Zhang, H.W.; Kako, T.; Ye, J.H. Highly efficient and stable photothermal catalytic CO₂ hydrogenation to methanol over Ru/In₂O₃ under atmospheric pressure. *Appl. Catal. B Environ.* **2023**, *327*, 122471. [[CrossRef](#)]
30. Dong, T.J.; Liu, X.Y.; Tang, Z.F.; Yuan, H.F.; Jiang, D.; Wang, Y.J.; Liu, Z.; Zhang, X.L.; Huang, S.F.; Liu, H.; et al. Ru decorated TiO_x nanoparticles via laser bombardment for photothermal co-catalytic CO₂ hydrogenation to methane with high selectivity. *Appl. Catal. B Environ.* **2023**, *326*, 122176. [[CrossRef](#)]
31. Li, J.L.; Sheng, B.W.; Qiu, L.; Yang, J.J.; Wang, P.; Li, Y.X.; Yu, T.Q.; Pan, H.; Li, Y.; Li, M.H.; et al. Photo-thermal synergistic CO₂ hydrogenation towards CO over PtRh bimetal-decorated GaN nanowires/Si. *Chem. Sci.* **2024**, *15*, 7714–7724. [[CrossRef](#)]
32. Zhai, J.; Xia, Z.; Zhou, B.; Wu, H.; Xue, T.; Chen, X.; Jiao, J.; Jia, S.; He, M.; Han, B. Photo-thermal coupling to enhance CO₂ hydrogenation toward CH₄ over Ru/MnO/Mn₃O₄. *Nat. Commun.* **2024**, *15*, 1109. [[CrossRef](#)]
33. Guo, C.; Tang, Y.; Yang, Z.; Zhao, T.; Liu, J.; Zhao, Y.; Wang, F. Reinforcing the efficiency of photothermal catalytic CO₂ methanation through integration of Ru nanoparticles with photothermal MnCo₂O₄ nanosheets. *ACS Nano* **2023**, *17*, 23761–23771. [[CrossRef](#)]
34. Jia, J.; O'Brien, P.G.; He, L.; Qiao, Q.; Fei, T.; Reyes, L.M.; Burrow, T.E.; Dong, Y.; Liao, K.; Varela, M.; et al. Visible and near-infrared photothermal catalyzed hydrogenation of gaseous CO₂ over nanostructured Pd@Nb₂O₅. *Adv. Sci.* **2016**, *3*, 1600189. [[CrossRef](#)] [[PubMed](#)]
35. Wang, Y.; Zhang, X.; Chang, K.; Zhao, Z.; Huang, J.; Kuang, Q. MOF Encapsulated AuPt Bimetallic Nanoparticles for Improved Plasmonic-induced Photothermal Catalysis of CO₂ Hydrogenation. *Chem. Eur. J.* **2022**, *28*, e202104514. [[CrossRef](#)]
36. Ge, H.; Kuwahara, Y.; Kusu, K.; Kobayashi, H.; Yamashita, H. Enhanced visible-NIR absorption and oxygen vacancy generation of Pt/H_xMoWO_y by H-spillover to facilitate photothermal catalytic CO₂ hydrogenation. *J. Mater. Chem. A* **2022**, *10*, 10854–10864. [[CrossRef](#)]
37. Gao, X.; Cao, L.; Chang, Y.; Yuan, Z.; Zhang, S.; Liu, S.; Zhang, M.; Fan, H.; Jiang, Z. Improving the CO₂ hydrogenation activity of photocatalysts via the synergy between surface frustrated Lewis pairs and the CuPt alloy. *ACS Sustain. Chem. Eng.* **2023**, *11*, 5597–5607. [[CrossRef](#)]
38. He, Z.H.; Li, Z.H.; Wang, Z.Y.; Wang, K.; Sun, Y.C.; Wang, S.W.; Wang, W.T.; Yang, Y.; Liu, Z.T. Photothermal CO₂ hydrogenation to hydrocarbons over trimetallic Co-Cu-Mn catalysts. *Green Chem.* **2021**, *23*, 5775–5785. [[CrossRef](#)]
39. Murthy, P.S.; Liang, W.B.; Jiang, Y.J.; Huang, J. Cu-Based Nanocatalysts for CO₂ Hydrogenation to Methanol. *Energy Fuels* **2021**, *35*, 8558–8584. [[CrossRef](#)]
40. Kho, E.T.; Tan, T.H.; Lovell, E.; Wong, R.J.; Scott, J.; Amal, R. A review on photo-thermal catalytic conversion of carbon dioxide. *Green Energy Environ.* **2017**, *2*, 204–217. [[CrossRef](#)]
41. Lou, D.; Xu, A.B.; Fang, Y.; Cai, M.; Lv, K.; Zhang, D.; Wang, X.; Huang, Y.; Li, C.; He, L. Cobalt-Sputtered Anodic Aluminum Oxide Membrane for Efficient Photothermal CO₂ Hydrogenation. *ChemNanoMat* **2021**, *7*, 1008–1012. [[CrossRef](#)]
42. Tang, Y.; Zhao, T.; Han, H.; Yang, Z.; Liu, J.; Wen, X.; Wang, F. Ir-CoO Active Centers Supported on Porous Al₂O₃ Nanosheets as Efficient and Durable Photo-Thermal Catalysts for CO₂ Conversion. *Adv. Sci.* **2023**, *10*, 2300122. [[CrossRef](#)]
43. Chen, G.; Gao, R.; Zhao, Y.; Li, Z.; Waterhouse, G.I.; Shi, R.; Zhao, J.; Zhang, M.; Shang, L.; Sheng, G.; et al. Alumina-supported CoFe alloy catalysts derived from layered-double-hydroxide nanosheets for efficient photothermal CO₂ hydrogenation to hydrocarbons. *Adv. Mater.* **2018**, *30*, 1704663. [[CrossRef](#)] [[PubMed](#)]
44. Song, C.Q.; Liu, X.; Xu, M.; Masi, D.; Wang, Y.G.; Deng, Y.C.; Zhang, M.T.; Qin, X.T.; Feng, K.; Yan, J.; et al. Photothermal Conversion of CO₂ with Tunable Selectivity Using Fe-Based Catalysts: From Oxide to Carbide. *ACS Catal.* **2020**, *10*, 10364–10374. [[CrossRef](#)]
45. Xiong, Y.; Chen, H.W.; Hu, Y.; Yang, S.Y.; Xue, X.L.; He, L.F.; Liu, X.; Ma, J.; Jin, Z. Photodriven Catalytic Hydrogenation of CO₂ to CH₄ with Nearly 100% Selectivity over Ag₂₅ Clusters. *Nano Lett.* **2021**, *21*, 8693–8700. [[CrossRef](#)] [[PubMed](#)]
46. Jiang, Z.; Yuan, Z.; Duchesne, P.N.; Sun, W.; Lyu, X.; Miao, W.; Viasus Pérez, C.J.; Xu, Y.; Yang, D.; Huang, B.; et al. A living photocatalyst derived from CaCu₃Ti₄O₁₂ for CO₂ hydrogenation to methanol at atmospheric pressure. *Chem. Catal.* **2023**, *3*, 100507. [[CrossRef](#)]
47. Xu, C.Y.; Huang, W.H.; Li, Z.; Deng, B.W.; Zhang, Y.W.; Ni, M.J.; Cen, K.F. Photothermal Coupling Factor Achieving CO₂ Reduction Based on Palladium-Nanoparticle-Loaded TiO₂. *ACS Catal.* **2018**, *8*, 6582–6593. [[CrossRef](#)]
48. Li, N.X.; Zou, X.Y.; Liu, M.; Wei, L.F.; Shen, Q.H.; Bibi, R.; Xu, C.J.; Ma, Q.H.; Zhou, J.C. Enhanced Visible Light Photocatalytic Hydrogenation of CO₂ into Methane over a Pd/Ce-TiO₂ Nanocomposition. *J. Phys. Chem. C* **2017**, *121*, 25795–25804. [[CrossRef](#)]

49. Fan, W.K.; Tahir, M. Current Trends and Approaches to Boost the Performance of Metal Organic Frameworks for Carbon Dioxide Methanation through Photo/Thermal Hydrogenation: A Review. *Ind. Eng. Chem. Res.* **2021**, *60*, 13149–13179. [[CrossRef](#)]
50. Zhou, J.; Liua, H.; Wang, H.Q. Photothermal catalysis for CO₂ conversion. *Chin. Chem. Lett.* **2023**, *34*, 107420. [[CrossRef](#)]
51. Lu, B.W.; Quan, F.J.; Sun, Z.; Jia, F.L.; Zhang, L.Z. Photothermal reverse-water-gas-shift over Au/CeO₂ with high yield and selectivity in CO₂ conversion. *Catal. Commun.* **2019**, *129*, 105724. [[CrossRef](#)]
52. Jiang, R.; Yue, X.; Wang, K.; Yang, Z.; Dai, W.; Fu, X. Photothermal-Catalyzing CO₂ Methanation over Different-Shaped CeO₂-Based Ru Nanoparticles. *Energy Fuels* **2022**, *36*, 11636–11646. [[CrossRef](#)]
53. Zhao, Z.Y.; Doronkin, D.E.; Ye, Y.H.; Grunwaldt, J.D.; Huang, Z.A.; Zhou, Y. Visible light-enhanced photothermal CO₂ hydrogenation over Pt/Al₂O₃ catalyst. *Chin. J. Catal.* **2020**, *41*, 286–293. [[CrossRef](#)]
54. Liu, H.M.; Shi, L.Z.; Zhang, Q.J.; Qi, P.; Zhao, Y.H.; Meng, Q.R.; Feng, X.Q.; Wang, H.; Ye, J.H. Photothermal catalysts for hydrogenation reactions. *Chem. Commun.* **2021**, *57*, 1279–1294. [[CrossRef](#)]
55. Li, Z.H.; Shi, R.; Ma, Y.N.; Zhao, J.Q.; Zhang, T.R. Photodriven CO₂ Hydrogenation into Diverse Products: Recent Progress and Perspective. *J. Phys. Chem. Lett.* **2022**, *13*, 5291–5303. [[CrossRef](#)] [[PubMed](#)]
56. He, X.; Liu, M.; Liang, Z.; Wang, Z.; Wang, P.; Liu, Y.; Cheng, H.; Dai, Y.; Zheng, Z.; Huang, B. Photo-enhanced CO₂ hydrogenation by plasmonic Cu/ZnO at atmospheric pressure. *J. Solid State Chem.* **2021**, *298*, 122113. [[CrossRef](#)]
57. He, J.H.; Lyu, P.; Jiang, B.; Chang, S.S.; Du, H.R.; Zhu, J.; Li, H.X. A novel amorphous alloy photocatalyst (NiB/In₂O₃) composite for sunlight-induced CO₂ hydrogenation to HCOOH. *Appl. Catal. B Environ.* **2021**, *298*, 120603. [[CrossRef](#)]
58. Lorber, K.; Djinic, P. Accelerating photo-thermal CO₂ reduction to CO, CH₄ or methanol over metal/oxide semiconductor catalysts. *iScience* **2022**, *25*, 104107. [[CrossRef](#)]
59. Lou, D.Y.; Zhu, Z.J.; Xu, Y.F.; Li, C.R.; Feng, K.; Zhang, D.K.; Lv, K.X.; Wu, Z.Y.; Zhang, C.C.; Ozin, G.A.; et al. A core-shell catalyst design boosts the performance of photothermal reverse water gas shift catalysis. *Sci. China Mater.* **2021**, *64*, 2212–2220. [[CrossRef](#)]
60. Mateo, D.; Morlanes, N.; Maity, P.; Shterk, G.; Mohammed, O.F.; Gascon, J. Efficient Visible-Light Driven Photothermal Conversion of CO₂ to Methane by Nickel Nanoparticles Supported on Barium Titanate. *Adv. Funct. Mater.* **2021**, *31*, 2008244. [[CrossRef](#)]
61. Ding, X.; Liu, X.; Cheng, J.H.; Li, D.; Li, T.F.; Jiang, Z.; Guo, Y. Boosted photothermal synergistic CO₂ methanation over Ru doped Ni/ZrO₂ catalyst: From experimental to DFT studies. *Fuel* **2024**, *357*, 129779. [[CrossRef](#)]
62. Wang, Z.M.; Xiao, M.Q.; Wang, X.X.; Wang, H.; Chen, X.; Dai, W.X.; Yu, Y.; Fu, X.Z. Thermo-driven photocatalytic CO₂ hydrogenation over NiO_x/Nb₂O₅ via regulating the electron transfer behavior of reactant gas adsorption. *App. Surf. Sci.* **2022**, *592*, 153246. [[CrossRef](#)]
63. Zhu, Z.J.; Hu, X.; An, X.D.; Xiao, M.D.; Zhang, L.; Li, C.R.; He, L. Photothermal Catalytic CO₂ Hydrogenation with High Activity and Tailored Selectivity Over Monodispersed Pd-Ni Nanoalloys. *Chem. Asian J.* **2022**, *17*, e202200993. [[CrossRef](#)]
64. Steeves, T.M.; Esser-Kahn, A.P. Demonstration of the photothermal catalysis of the Sabatier reaction using nickel nanoparticles and solar spectrum light. *RSC Adv.* **2021**, *11*, 8394. [[CrossRef](#)]
65. Li, Q.; Gao, Y.X.; Zhang, M.; Gao, H.; Chen, J.; Jia, H.P. Efficient infrared-light-driven photothermal CO₂ reduction over MOF-derived defective Ni/TiO₂. *Appl. Catal. B Environ.* **2022**, *303*, 120905. [[CrossRef](#)]
66. Li, J.R.; Xu, Q.; Han, Y.Y.; Guo, Z.Y.; Zhao, L.Q.; Cheng, K.; Zhang, Q.H.; Wang, Y. Efficient photothermal CO₂ methanation over NiFe alloy nanoparticles with enhanced localized surface plasmon resonance effect. *Sci. China Chem.* **2023**, *66*, 3518–3524. [[CrossRef](#)]
67. Kho, E.T.; Jantarang, S.; Zheng, Z.K.; Scott, J.; Amal, R. Harnessing the Beneficial Attributes of Ceria and Titania in a Mixed-Oxide Support for Nickel-Catalyzed Photothermal CO₂ Methanation. *Engineering* **2017**, *3*, 393–401. [[CrossRef](#)]
68. Li, Y.; Zeng, Z.J.; Zhang, Y.M.; Chen, Y.; Wang, W.J.; Xu, X.M.; Du, M.Y.; Li, Z.S.; Zou, Z.G. Deactivation and Stabilization Mechanism of Photothermal CO₂ Hydrogenation over Black TiO₂. *ACS Sustain. Chem. Eng.* **2022**, *10*, 6382–6388. [[CrossRef](#)]
69. Lv, C.C.; Bai, X.H.; Ning, S.B.; Song, C.X.; Guan, Q.Q.; Liu, B.; Li, Y.G.; Ye, J.H. Nanostructured Materials for Photothermal Carbon Dioxide Hydrogenation: Regulating Solar Utilization and Catalytic Performance. *ACS Nano* **2023**, *17*, 1725–1738. [[CrossRef](#)]
70. Canales, R.; Agirre, I.; Barrio, V.L. Ni-Fe nanoparticles prepared using hydrotalcite precursors enhance the photocatalytic performance of CO₂ methanation. *Int. J. Hydrogen Energy* **2024**, *56*, 1435–1445. [[CrossRef](#)]
71. He, Y.L.; Zhou, Y.; Feng, J.; Xing, M.Y. Photothermal conversion of CO₂ to fuel with nickel-based catalysts: A review. *Environ. Funct. Mater.* **2022**, *1*, 204–217. [[CrossRef](#)]
72. Ghossoub, M.; Xia, M.K.; Duchesne, P.D.; Segal, D.; Ozin, G. Principles of photothermal gas-phase heterogeneous CO₂ catalysis. *Energy Environ. Sci.* **2019**, *12*, 1122–1142. [[CrossRef](#)]
73. Fan, W.K.; Tahir, M. Recent developments in photothermal reactors with understanding on the role of light/heat for CO₂ hydrogenation to fuels: A review. *Chem. Eng. J.* **2022**, *427*, 131617. [[CrossRef](#)]
74. Zhao, S.H.; Li, C.H.; Ren, K.K.; Fang, Z.B.; Fang, P.; Zhu, Y.Y.; Fang, P.F. Ternary Ni-Co-Fe oxides based on Prussian blue analog for efficient photothermal catalytic CO₂ reduction to CO and CH₄. *Appl. Catal. A Gen.* **2023**, *655*, 119109. [[CrossRef](#)]
75. Zhang, F.; Li, Y.H.; Qi, M.Y.; Yamada, Y.M.A.; Anpo, M.; Tang, Z.R.; Xu, Y.J. Photothermal catalytic CO₂ reduction over nanomaterials. *Chem Catal.* **2021**, *1*, 272–297. [[CrossRef](#)]
76. Kattel, S.; Liu, P.; Chen, J.G.G. Tuning Selectivity of CO₂ Hydrogenation Reactions at the Metal/Oxide Interface. *J. Am. Chem. Soc.* **2017**, *139*, 9739–9754. [[CrossRef](#)] [[PubMed](#)]
77. Zhang, X.L.; Hu, S.; Zhang, F.Y.; Xing, S.C.; Hu, H.L.; Ye, J.H.; Wang, D.F. Tunable Selectivity of Photothermal CO₂ Reduction over Composition-Mediated Ni-Mo Alloy Catalysts. *Energy Technol.* **2024**, 2301505. [[CrossRef](#)]

78. Li, Q.; Wang, C.Q.; Wang, H.L.; Chen, J.; Chen, J.; Jia, H.P. Disclosing Support-Size-Dependent Effect on Ambient Light-Driven Photothermal CO₂ Hydrogenation over Nickel/Titanium Dioxide. *Angew. Chem. Int. Ed.* **2024**, *63*, e202318166. [[CrossRef](#)] [[PubMed](#)]
79. Zhu, X.L.; Zong, H.B.; Pérez, C.J.V.; Miao, H.H.; Sun, W.; Yuan, Z.M.; Wang, S.H.; Zeng, G.X.; Xu, H.; Jiang, Z.Y.; et al. Supercharged CO₂ Photothermal catalytic Methanation: High Conversion, Rate, and Selectivity. *Angew. Chem. Int. Ed.* **2023**, *62*, e202218694. [[CrossRef](#)]
80. Yang, G.X.; Wang, Q.; Kuwahara, Y.; Mori, K.; Yamashita, H. Recent Progress of Studies on Photoconversion and Photothermal Conversion of CO₂ with Single-Atom Catalysts. *Chem. Bio Eng.* **2024**, *1*, 289–311. [[CrossRef](#)]
81. Singh, S.; Verma, R.; Kaul, N.; Sa, J.; Punjal, A.; Prabhu, S.; Polshettiwar, V. Surface plasmon-enhanced photo-driven CO₂ hydrogenation by hydroxy-terminated nickel nitride nanosheets. *Nat. Commun.* **2023**, *14*, 2551. [[CrossRef](#)] [[PubMed](#)]
82. Song, X.X.; Gao, L.J.; Wu, M.Q.; Yuan, D.C.; Kang, X.X.; Lian, R.Q.; San, X.Y.; Li, Y.G. Atomically dispersed Ni catalyst to boost weak sunlight-driven CO₂ hydrogenation with 100% CO selectivity. *App. Surf. Sci.* **2023**, *609*, 155339. [[CrossRef](#)]
83. Jia, Z.W.; Ning, S.B.; Tong, Y.X.; Chen, X.; Hu, H.L.; Liu, L.Q.; Ye, J.H.; Wang, D.F. Selective Photothermal Reduction of CO₂ to CO over Ni-Nanoparticle/N-Doped CeO₂ Nanocomposite Catalysts. *ACS Appl. Nano Mater.* **2021**, *4*, 10485–10494. [[CrossRef](#)]
84. Zhao, T.T.; Yang, Z.Y.; Tang, Y.X.; Liu, J.R.; Wang, F.L. Advances and Perspectives of Photopromoted CO₂ Hydrogenation for Methane Production: Catalyst Development and Mechanism Investigations. *Energy Fuels* **2022**, *36*, 6711–6735. [[CrossRef](#)]
85. Zhu, Y.F.; Xie, B.Q.; Yuwono, J.A.; Kumar, P.; Sharma, A.S.; Nielsen, M.P.; Bendavid, A.; Amal, R.; Scott, J.; Lovell, E.C. Making light work: Designing plasmonic structures for the selective photothermal methanation of carbon dioxide. *EES Catal.* **2024**, *2*, 834–849. [[CrossRef](#)]
86. Fan, W.K.; Tahir, M.; Alias, H. Visible light promoted low temperature photothermal CO₂ methanation over morphologically engineered Ni/TiO₂ NWs catalyst. *Mater. Today Proc.* **2024**, *97*, 9–16. [[CrossRef](#)]
87. Li, P.; Zhang, S.L.; Xiao, Z.R.; Zhang, H.; Ye, F.; Gu, J.M.; Wang, J.D.; Li, G.Z.; Wang, D.S. Ni-TiO₂ catalysts derived from metal-organic framework for efficient photo-thermal CO₂ methanation. *Fuel* **2024**, *357*, 129817. [[CrossRef](#)]
88. Zhang, G.L.; Xu, Q.; Huang, H.; Zhou, F.; Yu, L.Y.; Chen, Q.; Yang, J.R.; Xiao, Y.L.; Zhang, Q. Ni-Doped In₂O₃ Photothermal Coupling Catalyzed Boosted Carbon Dioxide Hydrogenation to Methanol. *Ind. Eng. Chem. Res.* **2024**, *63*, 968–979. [[CrossRef](#)]
89. Liu, M.; Chen, G.; Song, Z.; He, Z.; Zhong, A.; Cui, M. Catalytic Dechlorination of Three Organochlorides by Recyclable Nano-Palladium-Engineered Natural Sponge with Formic Acid. *Catalysts* **2024**, *14*, 424. [[CrossRef](#)]
90. Ye, D.; Liu, L.; Peng, Q.; Qiu, J.; Gong, H.; Zhong, A.; Liu, S. Effect of Controlling Thiophene Rings on D-A Polymer Photocatalysts Accessed via Direct Arylation for Hydrogen Production. *Molecules* **2023**, *28*, 4507. [[CrossRef](#)]

Disclaimer/Publisher’s Note: The statements, opinions and data contained in all publications are solely those of the individual author(s) and contributor(s) and not of MDPI and/or the editor(s). MDPI and/or the editor(s) disclaim responsibility for any injury to people or property resulting from any ideas, methods, instructions or products referred to in the content.